Grunin *et al. Bioresour. Bioprocess.* (2020) 7:41
https://doi.org/10.1186/s40643-020-00332-8

Bioresources and Bioprocessing

RESEARCH Open Access

Cellulose–water system's state analysis by proton nuclear magnetic resonance and sorption measurements

Yuriy B. Grunin*, Leonid Yu. Grunin, Veronika Yu. Schiraya, Maria S. Ivanova and Daria S. Masas

Abstract

Most cellulose-based materials' manufacturing processes include processing this biopolymer in an aqueous medium. Sorption properties depend on cellulose supramolecular structure and nature of its change during moistening. Plenty of researchers' efforts have been directed to the development of scientifically sound and commercially reliable processes over the past decade for the cellulose fibers' dispersion in an aqueous medium. Therefore, it needs a more detailed study of the cellulose–water system components' interaction. This study presents the supramolecular structure and sorption properties of native cotton cellulose research results obtained by ^{1}H NMR relaxation, spectroscopy and sorption measurements. Hydrophilic properties of cellulose as an adsorbent are characterized, taking into account a porous system between its structural elements. We examine in detail water adsorption on the active surface of cellulose Iβ. We also demonstrate the approach for determining the entropy change in the first two layers of adsorbed water and estimate this value increased during adsorption. Cellulose moistening is accompanied by the decomposition of macrofibrils into microfibrils and is manifested in a crystallinity decrease and a specific surface area growth.

Keywords: Cellulose, Nuclear magnetic resonance, Adsorption, Supramolecular structure, Crystallinity

Introduction

Cellulose is one of the most common natural polymers with such essential properties as renewability and biodegradation (Li and Renneckar 2011; Grunin et al. 2012, 2015a; French 2017; Lindh et al. 2017). Cellulose and its derivatives are used as raw materials in many fields of industry and agriculture, pharmacy and medicine, in solving environmental problems and creating composite materials.

Due to the significance of cellulose use, many kinds of research are devoted to studying its structural organization and properties. We consider several essential models of cellulose structure and give a short outline of the researches of cellulose–water interaction using sorption measurements and nuclear magnetic resonance (NMR). The development of structural models is based on the results of studies of cellulose biosynthesis.

During the passage of glucose units through terminal complexes of the plasma membrane, chemical 1,4-β-glycosidic bonds form cellulose chains (Delmer and Amor 1995; Doblin et al. 2002; Brown 2004; Nishiyama et al. 2008; Nishiyama 2009; Grunin et al. 2012, 2015b). These cellulose chains aggregate into the elementary fibril (EF) by hydrogen bonds. EFs are being merged into microfibrils (MF) that in turn unite into macrofibrils. Each glucopyranose ring of cellulose chain inside of cellulose crystallites undergoes intra-, intermolecular and interlayer donor–acceptor hydrogen bonds. This increases the aggregation strength of cellulose chains and leads to the impossibility of penetration of water molecules into the depth of cellulose EFs (Nishiyama et al. 2002, 2003; Li and Renneckar 2011).

Based primarily on results of X-ray diffraction and electron microscopy measurements, at the end of sixties of

*Correspondence: GruninYB@volgatech.net
Volga State University of Technology, 3, Lenin Square, Yoshkar-Ola 424000, Russian Federation

the last century, most researchers preferred the crystalline–amorphous model of cellulose. This model included two types of cellulose structure scheme: with a straightened conformation of chains and with a folded structure of chains. The schemes proposed by Hess (Hess et al. 1958); (Mühlethaler 1969); (Fray-Wissling 1963), and (Tönnesen and Ellefsen 1960); Ono et al. (1997) were of the most important of the first type. One of the second types of schemes was shown in the research of Manley (1964). Researchers of that time preferred the scheme with a straightened conformation of cellulose chains. However, the above models have not been received the direct experimental confirmation.

Chanzy (1990) found that MFs of wood pulp, cotton and Valonia have a parallelepiped shape with a square cross-section. Verlhac et al. (1990) experimentally substantiated the dominant contribution of the cellulose surface layer to the formation of amorphous regions.

Currently, the layered model of cellulose MFs (Verlhac et al. 1990; Chanzy 1990; Baker et al. 2000; Viëtor et al. 2002; Nishiyama et al. 2002, 2003; Brown 2004; Kono and Numata 2006; Nishiyama 2009; Carpita 2011; Li and Renneckar 2011; Poletto et al. 2013; French et al. 2014) is highly popular.

Cellulose has permanent contact with water and reagents dissolved in it. Hence, the understanding of the interaction of water with cellulose is significant for the interpretation and prediction of cellulose response. Due to the complicated structure of cellulose, the mechanism of water adsorption in the cellulose–water system has studied by different physicochemical methods.

Many kinds of research aimed at studying the cellulose–water system involve the construction of sorption isotherms. However, an unambiguous interpretation of the nature of water adsorption on cellulose, described by various theories (Brunauer–Emmett–Teller (BET), Langmuir, Dubinin–Radushkevich, Henry), is still absent (Bikales and Segal 1971; Rowland 1980; Gregg and Sing 1982; Grunin et al. 2007; Lindman et al. 2010; Xie et al. 2011a; Grunin et al. 2013; Mihranyan et al. 2004; Hill et al. 2009; Xie et al. 2011b; Ceylan et al. 2012; Guo et al. 2017; Chen et al. 2018).

Mihranyan et al. (2004) presented the study results of water sorption on cellulose powders of various origins. Scanning electron microscopy, X-ray diffraction, moisture sorption and BET surface area analysis were applied for characterization of the structure of cellulose powders. Authors found that cellulose powders with higher crystallinity had lower moisture uptake at a relative humidity below 75%. The crystallinity of the highly dispersed cellulose sample measured by X-ray diffraction was 0.45 that corresponded to the crystallinity of elementary cellulose fibril (Grunin et al. 2018).

The water vapor sorption characteristics of natural fibers such as jute, flax, coir, cotton, hemp and Sitka spruce were studied by Hill et al. (2009). For isotherm fitting and estimation of water monolayer content, authors chose the Hailwood Horrobin model as fundamental.

Xie et al. (2011b) studied the water vapor sorption on cotton, filter paper, flax, hemp, jute, and sisal fibers. Results were analyzed by use of a parallel exponential kinetics model that was consisted of fast and slow sorption components. Authors showed that at the initial stage of desorption proceeded rather quickly and slowed down at lower relative pressures of water vapor. It could be explained due to difficulty in removing water from smaller micropores formed during the adsorption process.

As shown by Ceylan et al. (2012), the maximum sorption capacity decreased throughout the cotton fiber development. Authors also found that sorption properties of secondary wall of cotton compared with primary one in late periods of fibers maturation were worsened.

Effects of nanocellulose types caused by different preparation procedures on the total running time, equilibrium moisture content, sorption hysteresis, and sorption kinetics were examined by Guo et al. (2017). Authors showed that the amorphous fraction of cellulose nanofibers was more than that of cellulose nanocrystals. Therefore, the extent of structural swelling of cellulose nanofibers was more significant than with cellulose nanocrystals. Besides, the amorphous fractions of cellulose nanocrystals and nanofibers with cellulose II structure were more than for cellulose I structure.

Microscopic model of water sorption in cellulose was presented by Chen et al. (2018). The molecular mechanism responsible for hysteresis in sorption-induced swelling in cellulose was considered using atom-scale simulation. Authors established that moisture content and swelling exhibited hysteresis upon adsorption and desorption.

The use of NMR method has significantly expanded boundaries in the study of the supramolecular organization of cellulose and its hydrophilic properties, as well as cellulose–water system. The choice of the NMR method is related to its high information content, accuracy, ease of sample preparation and results' interpretation. Also, this method belongs to the category of nondestructive.

Atalla and Vanderhart (1984), studying cellulose samples by ^{13}C NMR, concluded that there are two crystalline cellulose allomorphs Iα and Iβ. Cellulose Iα has a one-chain triclinic unit cell, whereas cellulose Iβ has a two-chain monoclinic unit cell.

For investigating the structure of unlabeled cotton cellulose, Kirui et al. (2019) applied the natural abundance ^{13}C–^{13}C 2D correlation solid-state NMR spectroscopy,

as enabled by the sensitivity-enhancing technique of dynamic nuclear polarization. The authors characterized the change in the structural organization of allomorphs Iα and Iβ during ball-milling and showed the importance of large crystallite size for maintaining the Iα and Iβ model structures. Analyzing the high-field 2D ^{13}C–^{13}C correlation solid-state NMR spectra of ^{13}C-labeled plant primary cell walls, Wang et al. (2016) resolved seven cellulose structures, five of which corresponding to interior cellulose. Based on values of ^{13}C chemical shifts, authors concluded that most of these interior cellulose structures differed significantly from the Iα and Iβ structures found in crystalline cellulose of bacteria, algae, and animals.

Using ^{13}C NMR technique, Newman and Davidson (2004) examined surfaces of celluloses I and II. Authors concluded that the influence of hydroxymethyl conformation was stronger at C-4 than at C-6. The hydroxymethyl conformations at the cellulose–water interface were gauche–gauche on cellulose I and gauche-trans on cellulose II. Chemical shifts for C-4 in the crystallite cores of celluloses I and II differed by 0.2 ppm, meanwhile corresponding chemical shifts for crystallite surfaces differed by 3.0 ppm.

Bergenstråhle et al. (2008) presented the model of crystalline cellulose fibrils (a fibril aggregate). CP/MAS ^{13}C NMR data were confirmed that the C-4 peak doublet could derive from surfaces parallel to different crystallographic planes. Also, the doublet could originate from C-4 atoms located in surface anhydroglucose units with hydroxymethyl groups pointing either inward or outward.

Lindh et al. (2017) investigated the mobility of water molecules in ^{2}H-exchanged, and after that re-dried, microcrystalline cellulose by ^{2}H MAS NMR. Authors subtracted the spectral contribution of deuteroxyls from the spectrum of hydrated cellulose, thereby showing the existence of two distinct $^{2}H_2O$ spectral populations associated with mobile and immobile water environments. Those water phases were located on cellulose surfaces between and within microfibril aggregates, respectively.

Time-domain NMR is being used throughout many areas of science and technology. Time-domain NMR applications do not only cover research and development but also provide the organization of routine on-line and at-line procedures of quality assurance and quality control in production processes (Mitchell et al. 2014). The possibility of using ^{1}H NMR in the analysis of water adsorption on cellulose is shown in researches (Leisen et al. 2002; Banas et al. 2000; Taylor et al. 2008; Grunin et al. 2016, 2017, 2018).

Leisen et al. (2002) measured the entire adsorption/desorption isotherm at precisely defined levels of relative humidity using NMR data. This research presented the calculation of adsorbate parameters based on the analysis of sorption isotherm of water vapor on cotton cellulose fibers. At the relative pressure of water vapor of 75% on average, five layers of adsorbate were formed on a cellulose surface. The same result was obtained based on the modernized BET equation.

From the analysis of dependences of spin–lattice (T_1) and spin–spin (T_2) relaxation times on cellulose moisture content, Ono et al. (1997) proposed the structural scheme of cellulose, in which interfibrillar (meso) and intrafibrillar (micro) pores were provided. Moreover, in this scheme, the role of amorphous regions was played by surface layers of cellulose crystallites.

Banas et al. (2000) proposed the simple two-motion model of molecular dynamics based on the spin–lattice relaxation time dependencies on temperature and frequency for cellulose pulp. It was possible to find from the temperature dependence of spin–lattice relaxation time the values of correlation times and activation energies.

Taylor et al. (2008) showed that water in cellulose pores was present as multiple layers. Authors estimated thicknesses of water layers adsorbed on the cellulose surface using the Goldman–Shen pulse experiment.

Based on experiments on spin diffusion of nuclear magnetization, linear dimensions of the thickness of the surface of cellulose crystallites and the average depth of micropores formed between EFs as well as the process of their filling during water uptake were described (Grunin et al. 2017).

Even though the cellulose–water system was studied a lot, questions about the structural organization and properties of its components and the nature of interactions between them are still the object of discussion (Nishiyama et al. 2008; Taylor et al. 2008; Nishiyama 2009; Lindman et al. 2010; French et al. 2014; Lindman et al. 2017; French 2017; Grunin et al. 2018).

We aim this study both to summarize some argumentative points mentioned above and to analyze the physics of cellulose structural changes during water uptake, using TD-NMR measurements as well as adsorption data and thermodynamics calculations.

Materials and methods

Materials

The selection of objects for this study was aimed at eliminating the influence of lignin and hemicelluloses on measurement results. Therefore, the objects of study were samples of native cotton cellulose (GOST 595–79 Cotton cellulose. Specifications). Samples had the following characteristics: moisture regain at standard conditions —7%, density —1.54 g/cm^3, degree of polymerization —9000–15,000, crystallinity by X-ray Diffraction (average) —73%.

Methods

Adsorption

The isopiestic series method was used to construct adsorption isotherms of water vapor by cellulose samples (Grunin et al. 2015a). Samples with a height of 10 mm were placed in test tubes with an internal diameter of 8 mm. Samples preliminarily dried at 105 °C for 12 h were kept in desiccators with preset values of the relative pressure of water vapor to a constant weight at 20 °C.

Nuclear magnetic resonance

Measurements of ^{1}H NMR relaxation parameters of cellulose were carried out with an NMR analyzer (Spin Track, Resonance Systems, Russia) operating at 19 MHz for protons. The pulse sequence Free Induction Decay (FID) (Abragam 1961) was used to determine the spin–spin (transverse) relaxation times of cotton cellulose samples. The duration of 90° exciting radiofrequency pulse was selected automatically and was 2 μs. Each amplitude measurement was a result of averaging 50 scans. Time TR between scans was chosen according to the condition of equilibrium between the spin system and lattice $TR \geq 5T_1$ (T_1 is the spin–lattice relaxation time).

FID signals from moistened cotton samples were fitted by the function (Grunin et al. 2017, 2018):

$$\begin{aligned} \mathrm{FID}(t) =& A_1 \exp\left(-\frac{1}{2}a^2t^2\right)\cos\frac{1}{2}bt \\ &+ A_2\exp\left(-\frac{1}{2}M_2^{\mathrm{am}}t^2\right) + A_3\exp\left(-\left(\frac{t}{T_2^{*w}}\right)^2\right), \end{aligned} \tag{1}$$

where A_1, A_2, and A_3 are amplitudes of the short, medium, and long components of the signal, proportional to proton populations of the inner regions of crystallites, their surfaces, and adsorbed water molecules, respectively; M_2^{am} is the second moment of the Gaussian line from the amorphous sections; T_2^{*w} is characteristic spin–spin relaxation time of water molecules; a and b are coefficients those take into account the distribution of correlation times of the thermal motion of molecules.

The frequency-domain representation of the FID signal of moistened cellulose sample is shown in Fig. 3.

Since the amplitudes A_1 and A_2 are proportional to proton populations of the crystalline and amorphous phases of cellulose, the ratio of A_1 to the total number of hydrogen nuclei in cellulose sample allows calculating its crystallinity (Grunin et al. 2015a, 2015b, 2018):

$$k = \frac{A_1}{A_1 + A_2}. \tag{2}$$

The relation (2) was obtained under the assumption that surface molecules of cellulose crystallites form its amorphous regions.

The crystallinity of cotton cellulose was determined by X-ray diffraction analysis according to the Segal method (Segal et al. 1959) and IR-spectroscopy, according to the O'Connor and Nelson method (Nelson and O'Connor 1964). Results of estimating the crystallinity of cotton cellulose by these methods and formula (2) are in good agreement (Table 1).

We found (Grunin et al. 2012) that there is one molecule of mono-adsorbed water for one surface molecule of cellulose in the process of adsorption on average. This foundation gives us a reason to associate the crystallinity of cellulose k with the capacity of water monolayer w_m:

$$k = 1 - 9w_m. \tag{3}$$

Equating the right-hand sides of Eqs. (2, 3), we find that the capacity of the mono-adsorption layer of water can be calculated by the formula:

$$w_m = \frac{A_2}{9(A_1 + A_2)}. \tag{4}$$

Our studies showed that results of estimating the capacity of water monolayer using ^{1}H NMR (4) and the solution of the BET equation as applied to the adsorption isotherm coincide (Grunin et al. 2018).

Taking into account the effective cross-section of a water molecule ($10.5{\cdot}10^{-20}$ m^2) active specific surface area of cellulose S_{sp} (m^2/g) is determined by the equation (Grunin et al. 2015a, 2015b):

$$S_{sp} = 3500w_m. \tag{5}$$

Results and discussion

Structural model of native cotton cellulose

Existing structural models of cellulose explain many physicochemical properties. However, for a more detailed study of sorption properties of cellulose, it is necessary to take into account the formation of a porous system between structural elements and the distribution

Table 1 The crystallinity of cotton cellulose sample

Determination method	Crystallinity
NMR via formula (2)	0.75
X-ray diffraction according to the Segal method	0.79 (Bikales and Segal 1971), 0.7 (Shcherbakova et al. 2012)
IR-spectroscopy according to the O'Connor-Nelson method	0.71 (Bikales and Segal 1971)

of adsorption centers on cellulose active surface. Hence, the above structural models need to be clarified.

We propose the model of structural organization of cotton cellulose with the crystallinity of 0.7 (Fig. 1) based on the above review and results of our researches (Grunin et al. 2017, 2018). Cellulose macrofibril is formed by four partially co-crystallized MFs, each of which consists of four EFs, interconnected by relatively weak donor–acceptor hydrogen bonds. MF has an average transverse size of 60–80 Å and a length of up to several micrometers. The internal layered structure of EF is an alternation of aggregates of central and angular chains within the two-chain monoclinic unit cell (cellulose Iβ). The distance between adjacent EF layers in planes with the type (1,1,0), (− 1,− 1,0) and (− 1,1,0), (1,− 1,0) is 6 Å and 5.4 Å, respectively (Nishiyama et al. 2008; Li and Renneckar 2011). According to Dubinin's classification (Dubinin and Kadlec 1987), pores between structural elements of cellulose are classified as micro- and mesopores. This model allows visualizing the process of water adsorption on active cellulose surface.

Authors (Brown 2004; Verlhac et al. 1990; Nishiyama et al. 2003) proposed close variants of the supramolecular structure of cellulose. However, they did not take into account the specifics of the arrangement of cellulose chains, hydrophilic and hydrophobic regions of EF, and co-crystallization of EFs in MF.

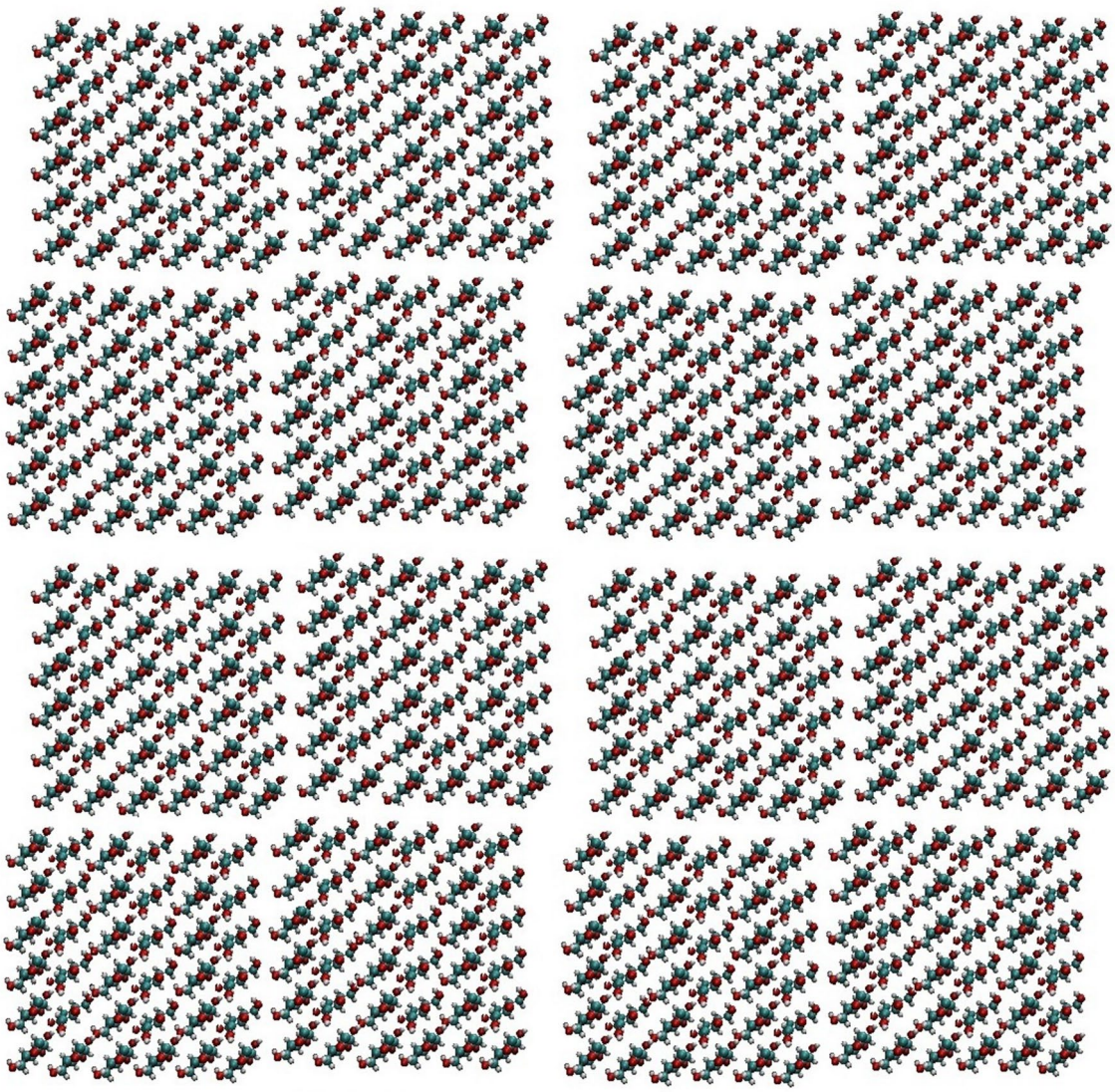

Fig. 1 Cross-sectional diagram of cellulose macrofibril, consisting of MF aggregates, each of which contains 4 EFs

The specificity of water adsorption process on cellulose

It was discussed (Grunin et al. 2013, 2018) that the penetrating and adsorption abilities of water molecules are stimulated by thermal motion and dipole–dipole interaction with surface-active centers (SAC) of cellulose. Surface hydroxyl groups of cellulose usually play the role of SACs. Based on simulations (Nishiyama et al. 2008; Nishiyama 2009) and atomic force microscopy data (Baker et al. 2000), our calculation shows that the distance between nearby SACs of cellulose is 6.5 Å in average.

The value of electric field strength of individual surface hydroxyl group E at the distance r from its center is calculated by the relation (Adamson and Gast 1997):

$$E = \frac{\mu'}{4\pi\varepsilon_0 r^3}\sqrt{3\cos^2\alpha + 1}, \tag{6}$$

where μ' is the –OH group electric dipole moment; α is the angle between the chosen direction and the axis of the dipole; r is the distance from the center of the dipole to the point of water molecule location; $\varepsilon_0 = 8.85 \times 10^{-12}$ F/m.

The surface hydroxyl group of cellulose has an electric dipole moment of 4.51×10^{-30} ℃ m, whereas water molecule has an electric dipole moment of 6.15×10^{-30} ℃ m (Gregg and Sing 1982).

Values of the module of electric field strength created by the SAC depending on distance are presented in Table 2 (calculations were performed for the case $\alpha = 0°$).

Based on data in Table 2, we assume that a high heterogeneity of electric field is enhanced by a large number of SACs in pores of cellulose.

The energy of the dipole–dipole interaction of water molecule with the individual surface hydroxyl group is given by the expression (Adamson and Gast 1997):

$$W = \mu E \cos\theta, \tag{7}$$

where μ is the electric dipole moment of the water molecule; θ is the angle between the vectors μ and E.

Table 2 The parameters of electric fields created by SACs of cellulose, depending on the distance

$r, m \times 10^{-10}$	$E, V/m \times 10^9$	W, kJ/mol
2.5	5.19	19.215
3	3.00	11.107
6	0.38	1.407
10	0.08	0.296
16	0.02	0.074
20	0.01	0.037

According to the data (Table 2), as a water molecule approaches an SAC of cellulose, their dipole–dipole interaction energy increases sharply and at the distance of 2.5–3 Å reaches the value of 19.2 kJ/mol, and it becomes commensurate with the energy of hydrogen bond of type –O–H···O– (Adamson and Gast 1997).

From our point of view, a water molecule can form the strong hydrogen bond during adsorption on cellulose Iβ in two ways. It will be carried out either by an oxygen atom of a water molecule on –OH group at C-6 of one glucopyranose ring or by two hydrogen atoms of a water molecule on O-2 and O-3 of an adjacent glucopyranose ring of same surface chain. It was discussed (Grunin et al. 2018) that this process is characteristic of each cellobiose residue of a surface chain of EF. From the previous, it follows that the adsorption monolayer is characterized by the relatively ordered arrangement of water molecules on the cellulose surface. Further equilibrium moistening of cellulose leads to the formation of subsequent adsorption layers (Taylor et al. 2008).

The adsorption process is characterized by an adsorption isotherm (Fig. 2), which up to 70% of relative pressure of water vapor is described by the BET equation satisfactorily:

$$w = w_m \frac{C \cdot p/p_s}{(1 - p/p_s) \cdot \left[1 + (C-1)p/p_s\right]}, \tag{8}$$

where w is the sample moisture content; C is the adsorption equilibrium constant; p/p_s is the relative pressure of water vapor.

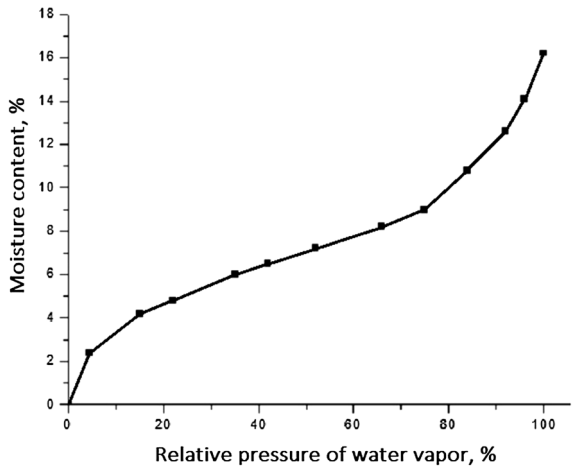

Fig. 2 Experimental adsorption isotherm of water vapor on cotton cellulose

Equation (8) allows examining the supramolecular structure and hydrophilic properties of cellulose and the state of water adsorbed on its fibers.

Being in adsorbed state, a water molecule experiences motions such as thermal rotational–vibrational and translational with jump-like character (Rowland 1980; Freeman 2003; Grunin et al. 2007). In the framework of the Bloembergen–Purcell–Pound theory (BPP), correlation times describe thermal motions of molecules that have Arrhenius character. This allows associating the activation energies of molecular motions with their correlation times in the first two layers of aqueous adsorbate (Grunin et al. 2016). For the first water adsorption layer:

$$\tau_1 = \tau_0 e^{\frac{\Delta H^0}{RT}}, \tag{9}$$

and for the second one:

$$\tau_2 = \tau_0 e^{\frac{L}{RT}}, \tag{10}$$

where ΔH^0 is the standard enthalpy of adsorption interaction; L is the heat of condensation of adsorbate; R is the universal gas constant; T is the absolute temperature; τ_1 and τ_2 are the correlation times of first and second adsorbate layers, respectively.

Dividing Eq. (10) by (9) and then taking the logarithm of the result, we get the expression for estimation the net heat of adsorption:

$$\Delta H^0 - L = RT \ln \frac{\tau_1}{\tau_2}. \tag{11}$$

In the framework of the BPP theory, correlation times in adsorbed water layers are related to their spin–spin relaxation times (under the condition $(\omega\tau)^2 \gg 1$, where ω is the circular NMR frequency, τ is the correlation time) by the formula (Grunin et al. 2016):

$$\frac{\tau_1}{\tau_2} = \frac{T_2^{(2)}}{T_2^{(1)}}, \tag{12}$$

where $T_2^{(1)}$ and $T_2^{(2)}$ are the true spin–spin relaxation times of first and second adsorbate layers, respectively. The measured spin–spin relaxation time of the first layer is equivalent to its true value due to the very slow proton exchange of cellulose with adsorbed water.

Finally, Eq. (11) takes the following form:

$$\Delta H^0 - L = RT \ln \frac{T_2^{(2)}}{T_2^{(1)}}. \tag{13}$$

We found the relation between the true spin–spin relaxation time of the second adsorption layer and the measured spin–spin relaxation time of adsorbed water bilayer (Grunin et al. 2020):

$$T_2^{(2)} = \frac{T_2^{(1)} \cdot T_{2\text{meas}}}{2T_2^{(1)} - T_{2\text{meas}}}, \tag{14}$$

where $T_{2\text{meas}}$ is the measured spin–spin relaxation time of adsorbed water bilayer.

The capacity of water monolayer was evaluated by solving the BET equation for the adsorption isotherm of water vapor on cotton cellulose (Fig. 2) and amounted to 0.032 g/g. The spin–spin relaxation time of water monolayer was estimated on cotton cellulose sample with moisture content close to the capacity of adsorption monolayer and amounted to 160 μs. The measured spin–spin relaxation time of adsorbed water bilayer was 280 μs. Hence, the ratio of true spin–spin relaxation times of second and first adsorption layers was 7. Substituting the above numerical values into the formula (13), we find that the net heat of adsorption is 4.87 kJ/mol. The value of net heat of adsorption is positive that indicates the dominance of the energy of water monolayer–adsorbent interaction over the condensation energy of adsorbate. The water monolayer–adsorbent interaction is carried out through the formation of hydrogen bonds. This entirely correlates with the above description of the scheme of water monomolecular adsorption on active cellulose surface.

Additional information on the state of adsorbed water can be obtained by analyzing the changing in entropy during adsorption.

The condition of thermodynamic equilibrium of water monolayer–water vapor can be written in the form of equality of total Gibbs free energy differentials (Gregg and Sing 1982):

$$V_v dp - S_v dT = V_m dp - S_m dT, \tag{15}$$

where V_v and V_m are the volumes of water vapor and water monolayer, respectively; S_v and S_m are the entropies of water vapor and water monolayer, respectively.

Transforming the formula (15), we get

$$(V_v - V_m)dp = (S_v - S_m)dT. \tag{16}$$

Since the volume of water vapor is much larger than the volume of water monolayer, at the initial stage of adsorption the water vapor can be considered as an ideal gas, then the left side of Eq. (16) is given as follows:

$$RT\frac{dp}{p} = (S_v - S_m)dT. \tag{17}$$

We transform the relation (17) into the following form:

$$R\frac{dp}{p} = \Delta H_1 \frac{dT}{T^2}. \tag{18}$$

where ΔH_1 is the enthalpy equivalent to the heat of mono-adsorption.

Carrying out the integration of Eq. (18), we get

$$RT(\ln p_1 - \ln p_0) = \Delta H_1, \tag{19}$$

where p_1 is the partial pressure of water vapor when filling water monolayer; p_0 is the additive integration constant.

Similarly, we obtain the expression for the integral heat of adsorption:

$$RT(\ln p_2 - \ln p_0) = \Delta H_2, \tag{20}$$

where p_2 is the partial pressure of water vapor when filling water bilayer; ΔH_2 is the enthalpy equivalent to the integral heat of adsorption.

We subtract Eq. (19) from (20):

$$RT \ln \frac{p_2}{p_1} = \Delta H_2 - \Delta H_1. \tag{21}$$

After transforming, the formula (21) is given as follows:

$$R \ln \frac{p_2}{p_1} = S_a - S_m, \tag{22}$$

where S_a is the entropy of water adsorbate.

Presenting the relation (22) with relative pressures of water vapor, we find

$$R \ln \frac{p_2}{p_s} \cdot \frac{p_s}{p_1} = S_a - S_m. \tag{23}$$

Thus, the excess of value p_2 over p_1 indicates the increase in the entropy change during adsorption. In particular, it is also valid for water bilayer adsorption under standard conditions. Analysis of the adsorption isotherm of water vapor on cotton cellulose (Fig. 2) shows that the filling of water monolayer is completed at p_1/p_s=11%; meanwhile, the filling of water bilayer is completed at p_2/p_s=42%. Applying the numerical values to Eq. (23) results that the difference between entropies of second and first adsorbed layers is 11.13 J/(K mol). This positive value indicates that water molecules in the first layer are more ordered than in the second one, which is in agreement with the above assumptions.

The adsorption equilibrium constant C is related to the change in Gibbs free energy by the Van't Hoff equation (Gregg and Sing 1982):

$$\Delta G^0 = -RT \ln C. \tag{24}$$

Since a part of the heat is released during adsorption, the change in entropy is related to the change in Gibbs free energy and the net heat of adsorption in accordance with the following expression (Grunin et al. 2016):

$$\Delta G^0 = \Delta H^0 - L + T\Delta S^0, \tag{25}$$

where ΔS^0 is the standard entropy of adsorbate.

Accordingly to the formula (25) and known numerical values, the change in Gibbs free energy is 8.21 kJ/mol.

After substituting relations (13, 23, 24) in (25), we get

$$RT \ln C = RT \ln \frac{T_2^{(2)}}{T_2^{(1)}} + RT \ln \frac{p_2}{p_s} \cdot \frac{p_s}{p_1}. \tag{26}$$

Consequently, the adsorption equilibrium constant can be estimated by the equation:

$$C = \frac{T_2^{(2)}}{T_2^{(1)}} \cdot \frac{p_2}{p_s} \cdot \frac{p_s}{p_1}. \tag{27}$$

Using the above numerical values, we establish that the adsorption equilibrium constant is 26.7. This value is in agreement with one that found by solving the BET equation (C=25).

Sorption process development often leads to supramolecular rearrangements of cellulose. In particular, we studied the effect of equilibrium moistening of cellulose on its crystallinity and the specific surface area. Cotton cellulose samples' crystallinities at different stages of moistening were estimated by the formula (2). Figure 3 shows the FID signal spectrum from the protons of air-dry cotton cellulose. According to Fig. 3, A_1 and A_2 are amplitudes values of (3) and (5) components, respectively.

Figure 4 shows the graph of the crystallinity of cotton cellulose versus its moisture content. The cellulose crystallinity decrease in the range from 0.78 to 0.70 is the

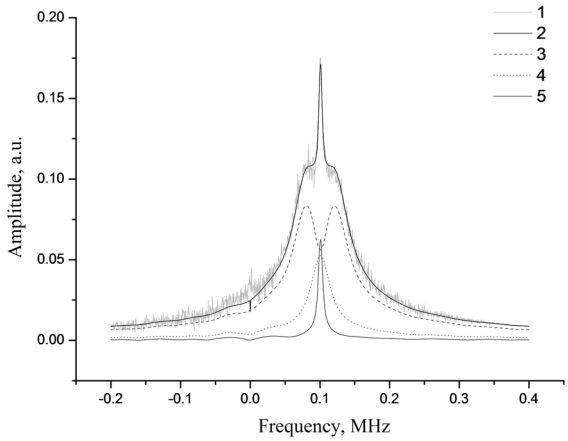

Fig. 3 Fourier transform spectrum of FID signal from protons of air-dry cotton cellulose: (1) original experimental spectrum, (2) simulated spectral line, (3) broad component, (4) medium component, and (5) narrow component

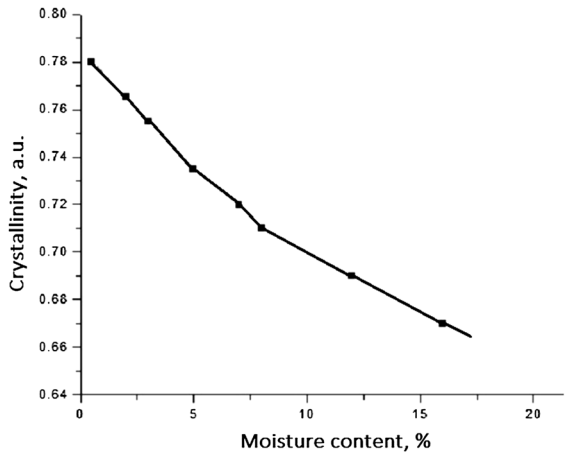

Fig. 4 Dependence the crystallinity of cellulose on its moisture content

most intensive with the corresponding moisture content from 0.5 to 8%. It is due to the thermal diffusion of water adsorptive molecules into spaces between MFs with subsequent adsorption on their active surfaces. This process is enhanced by the electric dipole–dipole interaction of adsorptive molecules with SACs of cellulose chains. As indicated above, the formation of –O–H···O– type hydrogen bond occurs. This phenomenon develops especially effectively in places of narrowing of pores between MFs and contributes to the formation of water adsorption layers and the occurrence of proppant pressure. Moreover, the distance increase between cellulose MFs results in the process of their separation and leads to the subsequent disintegration of macrofibril into MFs.

With the decrease in crystallinity from 0.7 to 0.67 with the corresponding moisture content in the range from 8 to 16%, adsorbed water molecules penetrate the structure of cellulose MFs. Water molecules break hydrogen bonds between co-crystallized EFs in the structure of MF adsorbing on active centers of their surfaces.

The work of adsorbed water penetration into spaces between crystalline cellulose formations is defined to a greater extent by the change in Gibbs free energy of the adsorption system. Hence, the proppant pressure from adsorbed water molecules Δp can be defined using the total differential of the Gibbs free energy under isothermal conditions (Adamson and Gast 1997):

$$\Delta p = \frac{\Delta G^0}{V}, \tag{28}$$

where V is the volume of 1 mol of liquid water.

Substituting the numerical values of ΔG^0 and V (18×10^{-6} m^3) into Eq. (28) results that the proppant pressure value is 4.56×10^8 Pa.

Due to the proppant pressure emerged from the side of adsorbed water molecules, the formation of additional active specific surface of moistened cellulose occurs. It varies from 77.5 to 128 m^2/g (using Eq. 5) in the moisture content range from 0.5 to 16% according to the adsorption isotherm (Fig. 2).

Conclusions

The model of the cellulose supramolecular structure is presented. It takes into account the crystallinity of cellulose and the presence of slit-shaped pores located between its structural elements. The scheme of specific adsorption of water molecules on the active surface of cellulose fibrils is proposed. The value of the net heat of adsorption is calculated based on the thermodynamic approach and characteristics of ^{1}H NMR relaxation in adsorption systems. The method for estimating the entropy change using relative pressures of water vapor is presented. The increase in entropy of adsorbate during equilibrium moistening of cellulose is established. It is shown that during the adsorption process the liquid adsorbate molecules diffuse into the co-crystallization zone of EFs in the structure of MF, which leads to the appearance of proppant pressure between them and dispersion of cellulose crystallites. It is presented that the equilibrium moistening of cellulose results to decrease in its crystallinity and increase in specific surface area.

Abbreviations

EF: Elementary fibril; MF: Microfibril; SAC: Surface active center; NMR: Nuclear magnetic resonance; FID: Free induction decay; BET: Brunauer–Emmett–Teller; BPP: Bloembergen–Purcell–Pound.

Acknowledgements

We thank Resonance Systems for providing "Spin Track" NMR Analyzer.

Authors' contributions

All authors performed material preparation, data collection and analysis. YG and MI wrote the first draft of the manuscript, which was translated by VS and commented by LG. YG was a major contributor in writing the manuscript. All authors read and approved the final manuscript.

Funding

This research did not receive any specific grant from funding agencies in the public, commercial, or not-for-profit sectors.

Availability of data and materials

All data generated or analyzed during this study are included in this published article.

Ethics approval and consent to participate

Not applicable.

Consent for publication

Not applicable.

Competing interests

The authors declare that they have no competing interests.

Received: 20 January 2020 Accepted: 7 July 2020
Published online: 15 July 2020

References

Abragam A (1961) The principles of nuclear magnetism. Clarendon Press, Oxford

Adamson AW, Gast AP (1997) Physical chemistry of surfaces. A Wiley-Interscience Publication, Canada

Atalla RH, Vanderhart DL (1984) Native celluloses: a composite of two distinct crystalline forms. Science 223:283–285. https://doi.org/10.1126/science.223.4633.283

Baker AA, Helbert W, Sugiyama J, Miles MJ (2000) New insight into cellulose structure by atomic force microscopy shows the Iα crystal phase at near-atomic resolution. Biophys J 79:1139–1145. https://doi.org/10.1016/S0006-3495(00)76367-3

Banas K, Blicharska B, Dietrich W, Kluza M (2000) Molecular dynamics of cellulose–water systems investigated by NMR relaxation method. Holzforschung 54:501–504. https://doi.org/10.1515/hf.2000.085

Bergenstråhle M, Wohlert J, Larsson PT, Mazeau K, Berglund LA (2008) Dynamics of cellulose–water interfaces: NMR spin-lattice relaxation times calculated from atomistic computer simulations. J Phys Chem B 112:2590–2595. https://doi.org/10.1021/jp074641t

Bikales NM and Segal L (eds) (1971) Cellulose and cellulose derivatives. Wiley-Interscience, New York

Brown RM (2004) Cellulose structure and biosynthesis: what is in store for the 21st century? J. Polymer Sci. Part A 42:487–495. https://doi.org/10.1002/pola.10877

Carpita NC (2011) Update on mechanisms of plant cell wall biosynthesis: how plants make cellulose and other (1 → 4)-β-D-glycans. Plant Physiol 155:171–184. https://doi.org/10.1104/pp.110.163360

Ceylan Ö, Van Landuyt L, Meulewaeter F, De Clerck K (2012) Moisture sorption in developing cotton fibers. Cellulose 19:1517–1526. https://doi.org/10.1007/s10570-012-9737-x

Chanzy H (1990) Aspects of cellulose structure. In: Kennedy JF, Phillips GO, Williams PA (eds) Cellulose Sources and Exploitation: industrial utilization biotechnology and physico-chemical properties. Ellis Horwood, New York

Chen M, Coasne B, Guyer R, Derome D, Carmeliet J (2018) Role of hydrogen bonding in hysteresis observed in sorption-induced swelling of soft nanoporous polymers. Nat Commun 9:3507–3513. https://doi.org/10.1038/s41467-018-05897-9

Delmer DP, Amor Y (1995) Cellulose biosynthesis. Plant Cell 7:987–1000. https://doi.org/10.1105/tpc.7.7.987

Doblin MS, Kurek I, Jacob-Wilk D, Delmer DP (2002) Cellulose biosynthesis in plants: from genes to rosettes. Plant Cell Physiol 43:1407–1420. https://doi.org/10.1093/pcp/pcf164

Dubinin MM, Kadlec O (1987) Novel ideas in the theory of the physical adsorption of vapors on micropore adsorbents. Carbon 25:321–324. https://doi.org/10.1016/0008-6223(87)90001-7

Fray-Wissling A (1963) The ultrastructure and biogenesis of native cellulose. Fortschr Chem Org Naturst 27:1–30

Freeman R (2003) Magnetic resonance in chemistry and medicine. Oxford University Press, USA

French AD (2017) Glucose, not cellobiose, is the repeating unit of cellulose and why that is important. Cellulose 24:4605–4609. https://doi.org/10.1007/s10570-017-1450-3

French AD, Concha M, Dowd MK, Stevens ED (2014) Electron (charge) density studies of cellulose models. Cellulose 21:1051–1063. https://doi.org/10.1007/s10570-013-0042-0

Gregg SJ, Sing KSW (1982) Adsorption, Surface Area and Porosity. ACADEMIC PRESS, London

Grunin YuB, Grunin LYu, Nikol'skaya EA (2007) Pulsed NMR method for determining the thermodynamic characteristics of adsorption processes in biopolymers. Russ J Phys Chem A 81:1165–1169. https://doi.org/10.1134/S003602440707028X

Grunin YuB, Grunin LYu, Nikol'skaya EA, Talantsev VI (2012) Microstructure of cellulose: NMR relaxation study. Polymer Science Ser A 54:201–208. https://doi.org/10.1134/S0965545X12030030

Grunin YuB, Grunin LYu, Nikol'skaya EA, Talantsev VI, Gogelashvili GSh (2013) Features of the sorption of water vapor and nitrogen on cellulose. Russ J Phys Chem A 87:100–103. https://doi.org/10.1134/S0036024413010093

Grunin LYu, Grunin YuB, Talantsev VI, Nikolskaya EA, Masas DS (2015a) Features of the structural organization and sorption properties of cellulose. Polymer Science Ser A 57:43–51. https://doi.org/10.1134/S0965545X15010034

Grunin YuB, Grunin LYu, Talantcev VI, Nikolskaya EA, Masas DS (2015b) Supramolecular reorganizations in cellulose during hydration. Biophysics 60:43–52. https://doi.org/10.1134/S0006350915010133

Grunin YuB, Grunin LYu, Masas DS, Talantsev VI, Sheveleva NN (2016) Proton magnetic relaxation study of the thermodynamic characteristics of water adsorbed by cellulose fibers. Russ J Phys Chem A 90:2249–2253. https://doi.org/10.1134/S003602441611008X

Grunin LY, Grunin YB, Nikolskaya EA, Sheveleva NN, Nikolaev IA (2017) An NMR relaxation and spin diffusion study of cellulose structure during water adsorption. Biophysics 62:198–206. https://doi.org/10.1134/S0006350917020087

Grunin YuB, Grunin LYu, Gal'braikh LS, Sheveleva NN, Masas DS (2018) Dispersion peculiarities of crystalline cellulose upon its moistening. Fibre Chem 49:321–326. https://doi.org/10.1007/s10692-018-9890-6

Grunin YuB, Ivanova MS, Masas DS, Grunin LYu (2020) Thermodynamics of adsorption in a cellulose-water system. Russ J Phys Chem A 94:704–708. https://doi.org/10.1134/S0036024420040056

Guo X, Wu Y, Xie X (2017) Water vapor sorption properties of cellulose nanocrystals and nanofibers using dynamic vapor sorption apparatus. Sci Rep 7:14207. https://doi.org/10.1038/s41598-017-14664-7

Hess K, Gütter E, Mahl H (1958) Die Ultratextur bei Fortisan. Elektronenmikroskopische Darstellung grosser Längsperioden in Zellulosefasern. Kolloid-Zeitschrift 158:115–119

Hill CAS, Norton A, Newman G (2009) The water vapor sorption behavior of natural fibers. J Appl Polym Sci 112:1524–1537. https://doi.org/10.1002/app.29725

Kirui A, Ling Z, Kang X, Dickwella Widanage MC, Mentink-Vigier F, French AD, Wang T (2019) Atomic resolution of cotton cellulose structure enabled by dynamic nuclear polarization solid-state NMR. Cellulose 26:329–339. https://doi.org/10.1007/s10570-018-2095-6

Kono H, Numata Y (2006) Structural investigation of cellulose I_α and I_β by 2D RFDR NMR spectroscopy: determination of sequence of magnetically inequivalent D-glucose units along cellulose chain. Cellulose 13:317–326. https://doi.org/10.1007/s10570-005-9025-0

Leisen J, Beckham HW, Benham M (2002) Sorption isotherm measurements by NMR. Solid State Nucl Magn Reson 22:409–422. https://doi.org/10.1006/snmr.2002.0069

Li Q, Renneckar S (2011) Supramolecular structure characterization of molecularly thin cellulose I nanoparticles. Biomacromol 12:650–659. https://doi.org/10.1021/bm101315y

Lindh EL, Terenzi C, Salmen L, Furo I (2017) Water in cellulose: evidence and identification of immobile and mobile adsorbed phases by ^{2}H MAS NMR. Phys Chem Chem Phys 19:4360–4369. https://doi.org/10.1039/C6CP08219J

Lindman B, Karlström G, Stigsson L (2010) On the mechanism of dissolution of cellulose. J Mol Liq 156:76–81. https://doi.org/10.1016/j.molliq.2010.04.016

Lindman B, Medronho B, Alves L, Costa C, Edlund H, Norgren M (2017) The relevance of structural features of cellulose and its interactions to dissolution, regeneration, gelation and plasticization phenomena. Phys Chem Chem Phys 19:23704–23718. https://doi.org/10.1039/C7CP02409F

Manley R (1964) Fine structure of native cellulose microfibrils. Nature 204:1155–1157. https://doi.org/10.1038/2041155a0

Mihranyan A, Llagostera AP, Karmhag R, Strømme M, Ek R (2004) Moisture sorption by cellulose powders of varying crystallinity. Int J Pharm 269:433–442. https://doi.org/10.1016/j.ijpharm.2003.09.030

Mitchell J, Gladden LF, Chandrasekera TC, Fordham EJ (2014) Low-field permanent magnets for industrial process and quality control. Prog Nucl Magn Reson Spectrosc 76:1–60. https://doi.org/10.1016/j.pnmrs.2013.09.001

Mühlethaler R (1969) Fine structure of natural polysaccharide systems. J Polymer Sci Part C. 28:305–316. https://doi.org/10.1002/polc.5070280124

Nelson ML, O'Connor RT (1964) Relation of certain infrared bands to cellulose crystallinity and crystal lattice type. Part I. Spectra of types I, II, III and

of amorphous cellulose. J Appl Polym Sci 8:1311–1324. https://doi.org/10.1002/app.1964.070080323
Newman RH, Davidson TC (2004) Molecular conformations at the cellulose–water interface. Cellulose 11:23–32. https://doi.org/10.1023/B:CELL.0000014778.49291.c6
Nishiyama Y (2009) Structure and properties of the cellulose microfibril. J. Wood Sci. 55:241–249. https://doi.org/10.1007/s10086-009-1029-1
Nishiyama Y, Langan P, Chanzy H (2002) Crystal structure and hydrogen-bonding system in cellulose Iβ from synchrotron X-ray and neutron fiber diffraction. J Am Chem Soc 124:9074–9082. https://doi.org/10.1021/ja025 7319
Nishiyama Y, Sugiyama J, Chanzy H, Langan P (2003) Crystal structure and hydrogen-bonding system in cellulose Iα from synchrotron X-ray and neutron fiber diffraction. J Am Chem Soc 125:14300–14306. https://doi.org/10.1021/ja037055w
Nishiyama Y, Johnson GP, French AD, Forsyth VT, Langan P (2008) Neutron crystallography, molecular dynamics, and quantum mechanics studies of the nature of hydrogen bonding in cellulose Iβ. Biomacromol 9:3133–3140. https://doi.org/10.1021/bm800726v
Ono H, Inamoto M, Okajima K, Yaginuma Y (1997) Spin-lattice relaxation behavior of water in cellulose materials in relation to the tablet forming ability of microcrystalline cellulose particles. Cellulose 4:57–73. https://doi.org/10.1023/A:1018415201945
Poletto M, Pistor V, Zattera AJ (2013) Structural Characteristics and Thermal Properties of Native Cellulose. In: Cellulose–Fundamental Aspects (Theo van de Ven and Louis Godbout, eds), IntechOpen
Rowland SP (ed) (1980) Water in polymers. ACS Symposium Series. American Chemical Societ, Washington
Segal L, Creely JJ, Martin AE, Conrad CM (1959) An empirical method for estimating the degree of crystallinity of native cellulose using the X-ray diffractometer. Text Res J 29:786–794. https://doi.org/10.1177/00405 1755902901003
Shcherbakova TP, Kotel'nikova NE, Bykhovtseva YuV (2012) Comparative study of powdered and microcrystalline cellulose samples of a various natural origins: physical and chemical characteristics. Russ J of Bioorg Chem 38:689–696. https://doi.org/10.1134/S1068162012070187
Taylor RE, French AD, Gamble GR, Himmelsbach DS, Stipanovic RD, Thibodeaux DP, Wakelyn PJ, Dybowski C (2008) ^{1}H and ^{13}C solid-state NMR of Gossypium barbadense (Pima) cotton. J Mol Struct 878:177–184. https://doi.org/10.1016/j.molstruc.2007.08.006
Tönnesen BA, Ellefsen O (1960) Chain folding—a possibility to be considered in connection with the cellulose molecule? Norsk Skogind. 14:266–269
Verlhac C, Dedier J, Chanzy H (1990) Availability of surface hydroxyl groups in valonia and bacterial cellulose. J Polymer Sci Part A 28:1171–1177. https://doi.org/10.1002/pola.1990.080280517
Viëtor RJ, Newman RH, Ha MA, Apperley DC, Jarvis MC (2002) Conformational features of crystal-surface cellulose from higher plants. Plant J. 30:721–731. https://doi.org/10.1046/j.1365-313x.2002.01327.x
Wang T, Yang H, Kubicki JD, Hong M (2016) Cellulose structural polymorphism in plant primary cell walls investigated by high-field 2D solid-state NMR spectroscopy and density functional theory calculations. Biomacromol 17:2210–2222. https://doi.org/10.1021/acs.biomac.6b00441
Xie Y, Hill CAS, Jalaludin Z, Sun D (2011a) The water vapour sorption behaviour of three celluloses: analysis using parallel exponential kinetics and interpretation using the Kelvin-Voigt viscoelastic model. Cellulose 18:517–530. https://doi.org/10.1007/s10570-011-9512-4
Xie Y, Hill CAS, Jalaludin Z, Curling SF, Anandjiwala RD, Norton A, Newman G (2011b) The dynamic water vapour sorption behaviour of natural fibres and kinetic analysis using the parallel exponential kinetics model. J Mater Sci 46:479–489. https://doi.org/10.1007/s10853-010-4935-0

Publisher's Note